RESONANT POWER CONVERTERS

Conventional pulse-width-modulated (PWM) switched-mode power converters (1) are used in many applications in industrial, aerospace, telecommunications, and consumer products. In these converters, power semiconductor switches are used as controlled switches to connect or to remove the input DC supply voltage to the output. With available fast switching devices, high-frequency (HF) magnetics and capacitors, and high speed control ICs, switching power converters have become very popular. In PWM switch-mode converters, square-wave pulse-width modulation is used for voltage regulation. The output voltage is varied by changing the duty cycle of the power semiconductor switch. The voltage (and current) waveform across the switch and at the output are square-wave and they generally result in higher switching losses when the switching frequency is increased. Also, the switching stresses are high with the generation of large electromagnetic interference (EMI) which is difficult to filter. However, these converters are easy to control, well understood, and have wide load and line control range. But to keep up with the developments in microelectronics, the general trend is to reduce the size, weight, and cost of power converters. This is achieved by increasing the switching frequency, which results in size reduction of magnetics (isolation transformer and filter inductors) and capacitors, whereas heat sink size is reduced by increasing the power conversion efficiency. Higher power efficiency is possible by reducing (or eliminating) the switching losses with resonant power conversion techniques.

In resonant power converters, an *LC* tank circuit(s) is added in the load circuit (or switched with auxiliary switches) to shape the load (and hence the switch) currents/voltages sinusoidally. This allows the power semiconductor switches to turn on or turn off at zero voltage or zero current, resulting in negligible switching losses. Some other advantages of resonant converters are that leakage inductances of HF transformers and the junction capacitances of semiconductors can be used profitably in the resonant circuit, and EMI is reduced. The major disadvantage of resonant converters, in general, is increased peak current (or voltage).

In the power converters discussed, when the dc input is converted to an HF ac, we call them resonant inverters. If the HF ac output is rectified and filtered to get a smooth dc output, then these power converters are called dc-to-dc resonant converters. Although resonant inverters and resonant dc-to-dc converters have many operating similarities, their actual analysis and design differ. Resonant inverters are discussed first.

LOAD RESONANT INVERTERS

Figure 1(a) shows the half-bridge resonant inverter circuit with a generalized tank circuit and load (2,3) connected across terminals A and B. A center-tapped dc source is created by two large smoothing capacitors connected across the dc supply. A square-wave voltage is generated across terminals A and B, by connecting sources V_1 and V_2 ($V_1 = V_2 = E = V_s/2$) alternately [Fig. 1(b)] using the switch-diode pairs, S_1, D_1 and S_2, D_2. Although MOSFETs are shown as the switches S_1 and S_2, other switching power devices (e.g., bipolar power transistors, insulated gate bipolar transistors (IGBTs), SCRs, gate turn-off (GTO) thyristors are also used. If SCRs are used as the switching devices, then a forced commutation circuit is needed unless natural or load commutation takes place. The diodes D_1 and D_2 provide the path for the reactive current.

If the load (including the tank circuit) across AB is an *RLC* type as shown in Fig. 1(c), then the inverter is called a *series-resonant inverter* or *series-loaded resonant inverter*. The components L and C are part of the load circuit or are added externally. Usually, a HF transformer is added for voltage scaling or isolation, and Fig. 1(d) shows the series-loaded resonant inverter circuit including the HF transformer. There are several other resonant tank circuit configurations possible which generate many inverter topologies (3). Among them,

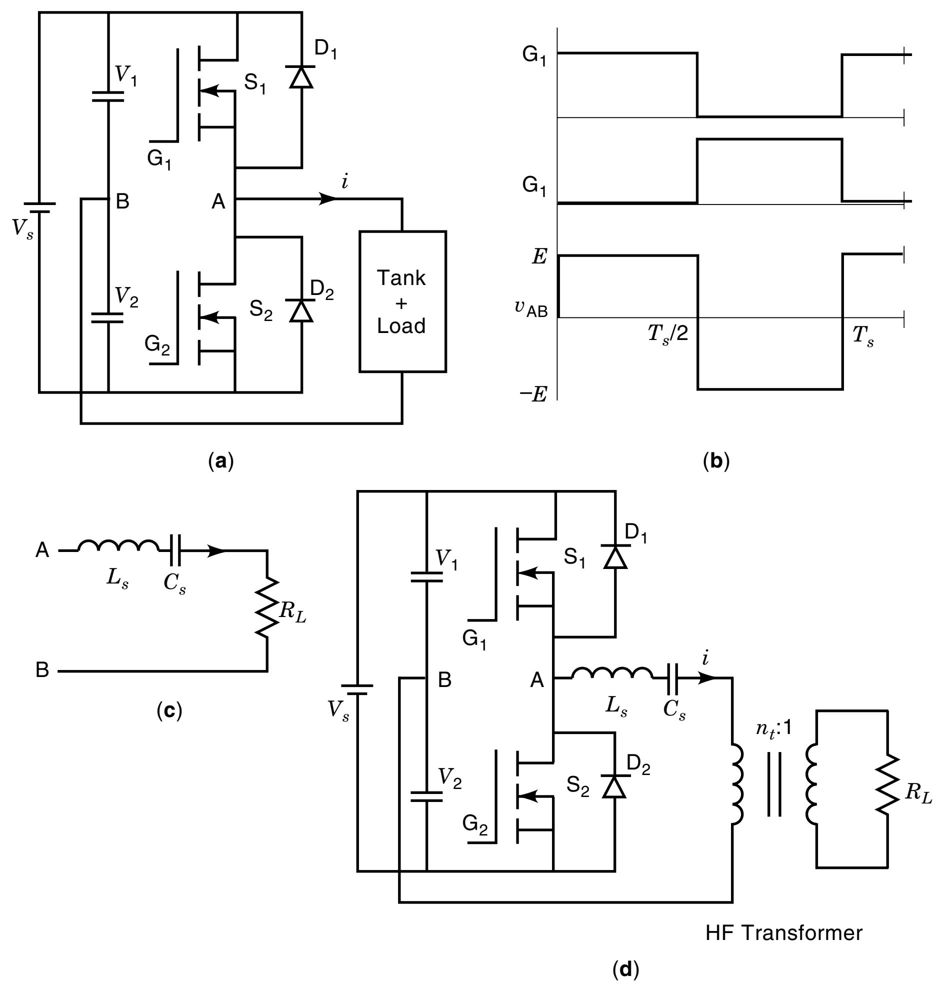

Figure 1. (a) Basic circuit diagram of a half-bridge load resonant inverter configuration with a generalized tank circuit. Snubber circuits are not shown. $V_1 = V_2 = E = V_s/2$. (b) Gating pulses and the voltage v_{AB}. (c) *RLC* circuit connected across AB to realize a series-loaded resonant inverter. (d) High-frequency, transformer-isolated, series-loaded resonant inverter.

two more popular configurations are parallel-loaded or parallel-resonant inverters [Fig. 2(a)], and *series-parallel* (or LCC-type) inverters [Fig. 2(b)]. For high-power applications, full-bridge inverters are used. A series-loaded, full-bridge resonant inverter is shown in Fig. 3. Its behavior is similar to a half-bridge except that the amplitude of output voltage v_{AB} is supply voltage V_s. Therefore, for the same output power, the peak current through the switches is half compared with the half-bridge inverter.

Operation

The current wave shape depends on whether the circuit across the output AB is underdamped or overdamped. Two types of operation (described for half-bridge) possible are discussed here (2–5).

Case 1, Zero-Current-Switching or Below-Resonance (Leading Power Factor) Mode of Operation. The inverter operates in this mode when the load across A and B (i.e., the tank circuit together with the load) is underdamped and Fig. 4(a) shows the typical steady-state operating waveforms. The sequence of device conduction is also shown in the same figure. Assume that the switch S_1 is carrying the load current. Because an underdamped *RLC* circuit is used, the current is approximately sinusoidal. At $t = t_1$, current goes to zero naturally and tries to reverse. Switch S_1 turns off and diode D_1 starts conducting providing the path for the reverse current. During the conduction by D_1 (or D_2), a reverse voltage from a diode drop is applied across S_1 (or S_2). This time t_q for which the diode conducts must be greater than the turn-off time t_{off} of the switch for successful operation of the circuit. At the end of the half-cycle, that is, at $t = T_s/2$ (where T_s is the period of the waveform equal to $1/f_s$ and f_s is the switching frequency), S_2 is turned on. In an ideal switch-diode pair, S_2 turns on immediately applying a reverse voltage across D_1. Therefore, D_1 turns off and S_2 carries the load current. When the current through S_2 goes to zero, D_2 conducts, and the cycle is complete when S_1 is turned on at the beginning of the next cycle.

In this type of operation, the switches turn off naturally, that is, load commutation takes place. This means that SCRs can be employed provided that the turn-off time condition mentioned previously (that is, $t_q > t_{off}$) is satisfied. Also note the following:

1. The switches turn off with zero current. Therefore, this operation is called *zero-current switching* (ZCS) and there are no turn-off losses.
2. The load current i leads the voltage across AB, which is why this type of operation is called the leading PF mode

of operation. In practice, the switching frequency is usually below the resonance frequency of the *RLC* circuit. Hence, it is also called *operation below resonance.*

The turn-on time of the switch and the reverse recovery time of the diode have been neglected in the explanation given previously. But in practice, this is not true and because of the reverse recovery time of the diode, when a switch in the other arm is turned on, the conducting diode does not turn off instantly. This results in a short interval during which the turned-on switch and the reverse-conducting diode short circuit the supply voltage. To take care of this, *di/dt* limiting inductors (L_1) are connected in series with each switch. Figure 4(b) illustrates this for the series-loaded resonant inverter. Fast recovery diodes are used to reduce the size of these extra inductors and to reduce the losses. If switches with slow recovery internal diodes (e.g., MOSFETs) are used, then the internal diodes must be bypassed by connecting external fast recovering diodes as shown in Fig. 4(b).

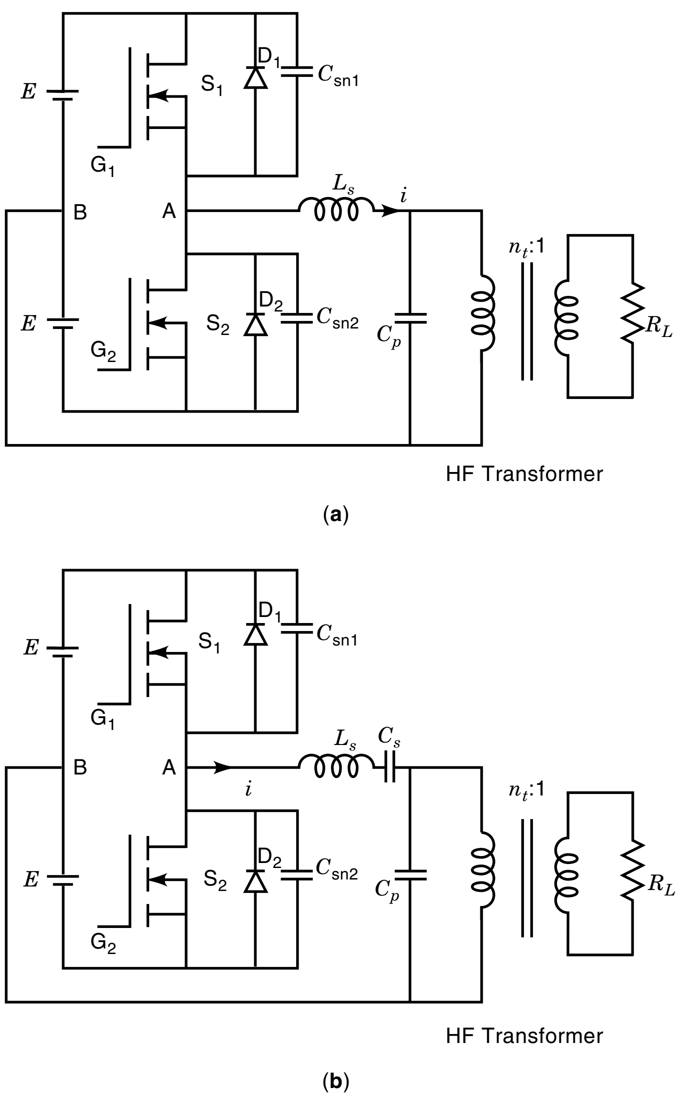

Figure 2. (a) Parallel-loaded resonant inverter. (b) Series-parallel-loaded (or LCC-type) resonant inverter.

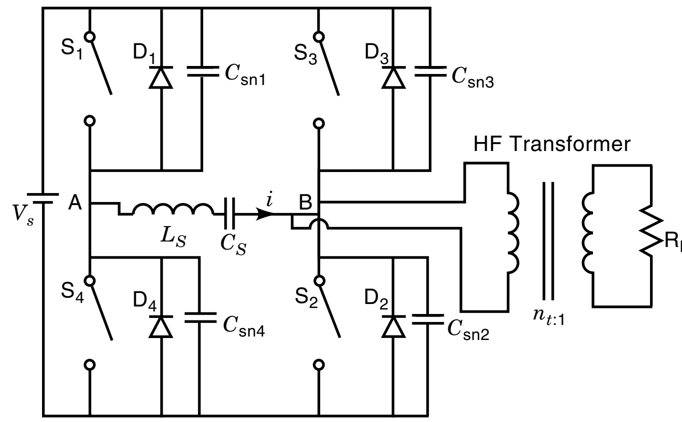

Figure 3. Basic circuit diagram of a full-bridge, series-loaded, resonant inverter.

The rate of rise of voltage *dv/dt* is limited by connecting a snubber capacitor (C_{sn}) across each switch. When a switch is conducting, the capacitor across the other switch is charged to the supply voltage V_s. This capacitor discharges when the switch across it is turned on resulting in a large peak current through the switch. To limit this peak current, a resistor (R_{sn}) is connected in series with each snubber capacitor. The power rating of these snubber resistors is equal to $C_{sn}V_s^2f_s$, that is, losses in these snubber resistors increase if the switching frequency or the supply voltage increases.

Case 2, Zero-Voltage-Switching or Above-Resonance (Lagging PF) Mode of Operation. The gating signals and the steady-state waveforms for this mode of operation, shown in Fig. 5, occur when the *RLC* circuit [Fig. 1(c)] is overdamped. Assume that D_1 is conducting. The current through D_1 goes to zero at t_1, and the load current reverses after this. Because the gating signal is already applied to S_1, current is transferred to S_1. Because the antiparallel diode across S_1 was conducting just before S_1 turns on, S_1 turns on with *zero-voltage switching* (ZVS). This means there are no turn-on losses. The switch S_1 is turned off at $T_s/2$, and the current through the load is transferred to D_2. The next half-cycle is similar to the first half-cycle. When S_1 or S_2 is turned off, snubber capacitor across the switch starts charging during the turn-off time of the switch, whereas the snubber capacitor across the incoming diode starts discharging from the supply voltage. Because C_{sn1} and C_{sn2} are in series and directly across the supply, the sum of the voltages across these two capacitors must be equal to the supply voltage at any time. Therefore, the diode across the discharged capacitor starts conducting when the voltage across the turned-off switch reaches V_s. The charging and discharging current of the capacitors flow through the load circuit. By properly choosing these snubber capacitors, the turn-off losses are minimized.

With this type of operation, lossy snubbers and *di/dt* inductors are not required, that is, only a capacitive snubber is used across the switch. Because there is enough time for the diodes to recover, internal diodes of MOSFETs, IGBTs (if antiparallel diodes are built in), and bipolar transistors are also used. Because the switches are turned off forcibly, how-

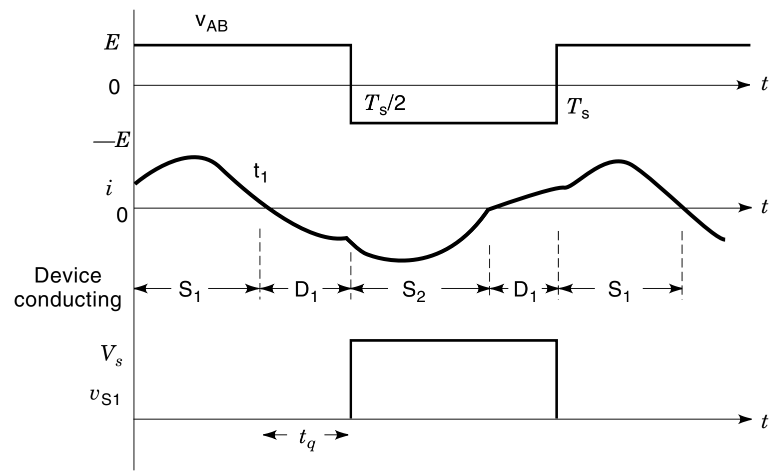

(a)

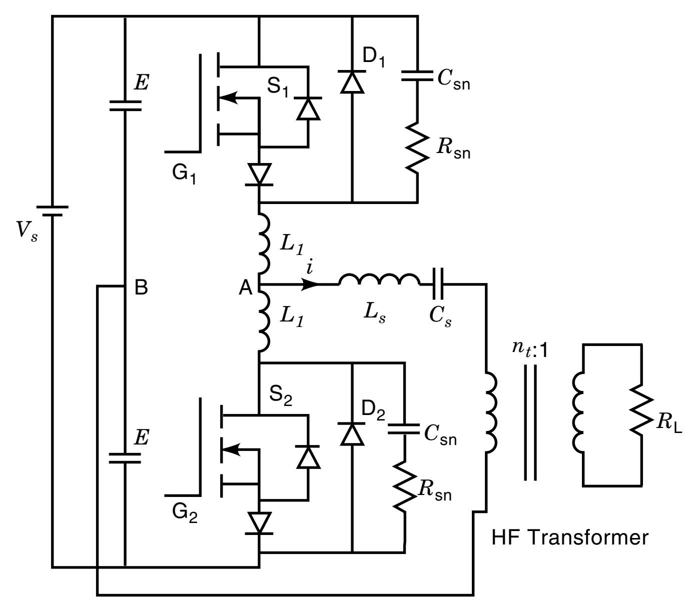

(b)

Figure 4. (a) Operating waveforms of the half-bridge configuration [Fig. 1(a)] for below resonance (or leading PF) mode of operation. (b) Half-bridge configuration with the di/dt inductors (L_1, L_1) and snubber components suitable for below resonance operation.

ever, a forced commutation circuit is required if SCRs are used as switches.

Power control for resonant inverters is achieved either by variable-frequency control or fixed-frequency control. Fixed-frequency control is not applicable to the half-bridge configuration (but is used in a full-bridge inverter, as discussed later), and therefore, only variable-frequency control is explained next.

The inverter operates near the resonance frequency at full load and minimum input voltage. In this case, the switching frequency is varied for power control. The following two possibilities exist:

1. At full load and minimum input voltage, the switching frequency is slightly below resonance but enough turn-off time for the switches is provided. As the load current decreases or the input voltage increases, the inverter switching frequency is decreased below this value. If the switching frequency is reduced below a certain value, the resonant current becomes discontinuous (Fig. 6). In addition to the disadvantages of below-resonance operation mentioned earlier, this control method has an additional disadvantage, namely, the magnetics and input/output filters have to be designed for the lowest frequency of operation, which increases the inverter size.

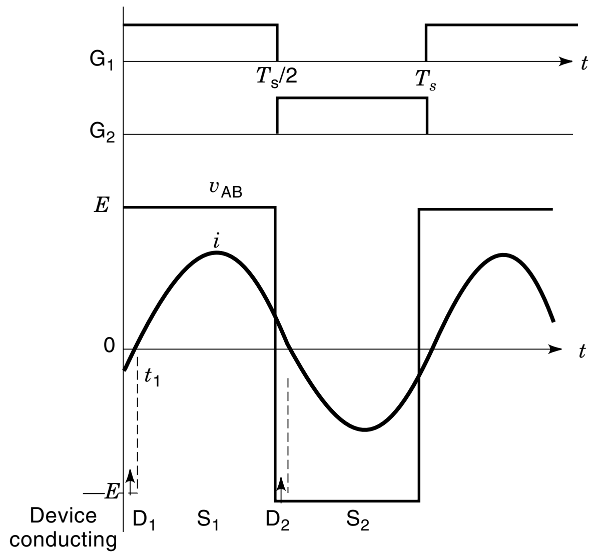

Figure 5. Operating waveforms of the half-bridge load resonant inverter [Fig. 1(a)] for above resonance (or lagging PF) mode of operation.

2. At full load and minimum input voltage, the switching frequency is slightly above the resonance frequency. Power is controlled by increasing the switching frequency above this value. This method has all of the advantages of above-resonance operation explained earlier. Also, the inverter always operates in a continuous current mode. SCRs cannot be used in this case because forced commutation or gate turn-off capability is required. The switching frequency required is also very high at light load conditions, which increases the magnetic core losses and makes the control circuit design difficult.

Analysis

Differential Equations (or Time-Domain Analysis) Approach. In this method, differential equations for the load circuit during different intervals are written and they are solved to obtain solutions for various state variables. This method is useful when the transient response of the inverter has to be predicted. Steady-state solutions are obtained by matching the boundary conditions at the end of various intervals. This approach is complex when the order of the load circuit is higher.

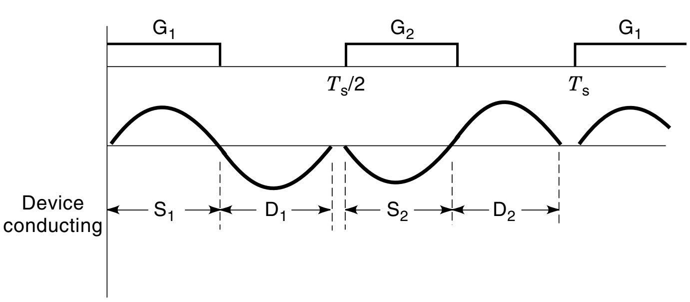

Figure 6. Discontinuous current mode of operation for a resonant inverter.

Frequency-Domain Analysis. Under steady-state conditions, the Fourier series expressions are written taking into account all of the harmonics or using only the fundamental componet in the simplified approximate analysis.

Fourier-Series Approach. In this approach (3), the square-wave voltage across AB is represented by the Fourier series (note: $E = V_s/2$ for half-bridge and $E = V_s$ for full-bridge; $\omega_s = 2\pi f_s$):

$$v_{\mathrm{AB}} = (4E/\pi) \sum_{n=1,3}^{\infty} [\sin(n\omega_s t)/n] \tag{1}$$

The nth harmonic phasor equivalent circuits across AB for the series-loaded and series-parallel-loaded resonant inverters are shown in Fig. 7(a) and (b), respectively. Using this circuit, the nth harmonic voltage and current equations can be written. Then the effect of all the harmonics are superposed to obtain the total response. In Fig. 7, the nth harmonic of the output voltage and the load resistor are referred to the primary side (using the turns ratio n_t of the transformer) and are denoted by V'_{on} $(= n_t V_{\mathrm{on}})$ and R'_L $(= n_t^2 R_L)$, respectively.

The current at the output of the inverter is given by

$$i = [4E/\pi] \sum_{n=1,3}^{\infty} [\sin(n\omega_s t - \phi_n)/(nZ_n)] \tag{2}$$

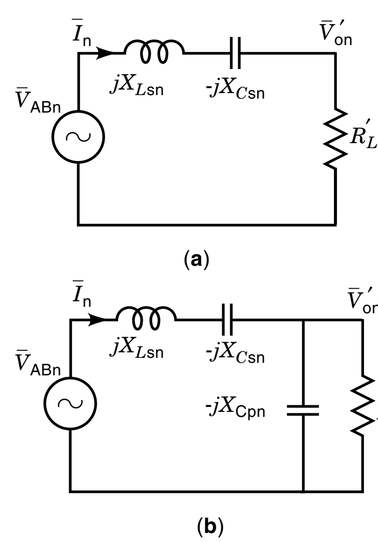

Figure 7. Phasor circuits for nth harmonic for (a) series-loaded resonant inverter and (b) series-parallel resonant inverter. $\overline{V}_{\mathrm{ABn}}$ and $\overline{V}'_{\mathrm{on}}$ are the nth harmonic phasors of voltage v_{AB} and the output voltage referred to the primary side of the high-frequency transformer, respectively. $\overline{I}_n$ is the nth harmonic phasor current at the output of the resonant inverter. $X_{L\mathrm{sn}} = n\omega_s L_s$, $X_{C\mathrm{sn}} = 1/(n\omega_s C_s)$, and $X_{Cpn} = 1/(n\omega_s C_p)$ are the nth harmonic reactances of L_s, C_s, and C_p, respectively.

where Z_n is the impedance across terminals A and B. For example, for a series-loaded resonant inverter

$$Z_n = \{R_L'^2 + [n\omega_s L_s - 1/(n\omega_s C_s)]^2\}^{1/2} \tag{3}$$

and

$$\phi_n = \tan^{-1}\{[n\omega_s L_s - 1/(n\omega_s C_s)]/R_L'\} \tag{4}$$

The voltage and current through other components are obtained similarly.

Approximate Analysis Approach. In this method, all of the harmonics except the fundamental are neglected (2,4,6,7). Although the method is an approximate approach, it is used to design an inverter simply. The fundamental voltage across AB is given by

$$v_{\mathrm{AB}} = (4E/\pi)[\sin(\omega_s t)] \tag{5}$$

Then the current at the output of the inverter is expressed as

$$i = [4E/(\pi Z_1)][\sin(\omega_s t - \phi_1)] \tag{6}$$

The value of ϕ_1 determines whether the inverter is operating in the lagging or leading PF mode (2). If ϕ_1 is negative, the initial current (i at $t = 0$) is positive, and the inverter is operating in the leading PF mode. If ϕ_1 is positive, the initial current is negative and the inverter is operating in the lagging PF mode, and forced commutation is necessary.

Using the approximate analysis, the gain of resonant inverters is derived easily. The following base quantities are used for normalizing the equations:

Base voltage: $V_B = E$ where $E = V_s/2$ for half-bridge and V_s for full-bridge
Base impedance: $Z_B = R_L' = n_t^2 R_L$
Base current: $I_B = V_B/Z_B$

For a series loaded resonant inverter, considering only the fundamental component and neglecting all the harmonics, [Fig. 7(a), with $n = 1$],

$$M(j\omega_s) = V_{O1}'/V_{\mathrm{AB1}} = \frac{R_L'}{R_L' + j[w_s L_s - (1/w_s C_s)]} \tag{7}$$

$$M = |M(j\omega_s)| = 1/[1 + (Q_s F - Q_s/F)^2]^{1/2} \quad \text{p.u.} \tag{8}$$

where

$$Q_s = (L_s/C_s)^{1/2}/R_L', F = \omega_s/\omega_r$$
$$\omega_s = 2\pi f_s$$

and

$$\omega_r = 1/(L_s C_s)^{1/2}$$

Similarly, for a parallel-loaded resonant inverter,

$$M = 1/[(1 - F^2)^2 + (F/Q_p)^2]^{1/2} \quad \text{p.u.} \tag{9}$$

where

$$Q_p = R_L'/(L_s/C_p)^{1/2}$$
$$F = \omega_s/\omega_p$$

and

$$\omega_p = 1/(L_s C_p)^{1/2}$$

and, for a series-parallel resonant inverter,

$$M = 1/\{[1 + (C_p/C_s)(1 - F^2)]^2 + (Q_s F - Q_s/F)^2\}^{1/2} \quad \text{p.u.} \tag{10}$$

In the case of a series resonant inverter, L_s includes the leakage inductance of the HF transformer. For parallel and series-parallel resonant inverters, leakage inductance is made part of L_s by placing the resonant capacitor C_p across the secondary winding of the HF transformer.

The equations previously derived were used in MATHCAD to obtain the plots of inverter gain versus frequency ratio F for the three resonant inverters and are shown in Fig. 8. The figure shows that the frequency variation required for load regulation is very wide for a series-loaded inverter, whereas it is very narrow for a parallel-loaded resonant inverter. But the inverter's switch-peak current decreases with the load current for a series-loaded inverter, whereas it does not decrease with the load current in a parallel-loaded resonant inverter. The series-parallel resonant inverter combines the advantages of series-loaded and parallel-loaded resonant inverters. Also, with proper selection of the C_s/C_p ratio, a near sine-wave output waveform almost load-independent is obtained.

The resonant inverters previously discussed use voltage-source input and are therefore voltage-source resonant inverters. If a constant current-source input is used, then one can implement a current-source resonant inverter. This type of inverters is discussed in (5).

Resonant inverters are particularly useful in generating high-frequency voltage waveforms. They are used in induction heating, fluorescent lamp electronic ballasts, and other applications. In electronic ballasts, HF ac (of the order of 20 kHZ) is used to feed the fluorescent lamp instead of 60 Hz ac. This approach reduces the ballast size and also gives more light output. Induction heating is used for surface hardening or annealing. In Fig. 1(d), if the material to be heated forms the secondary coil (the inductance on primary side is removed), then HF currents are induced in the metal piece forming the secondary circuit. The skin depth or penetration depth δ is given by

$$\delta = k(\rho/f_s)^{1/2} \tag{11}$$

where ρ is the resistivity of the material, f_s is the HF supply frequency (i.e., the switching frequency of the inverter), and k is a constant. If low frequency is used, then the metal piece can be melted. A current-fed parallel resonant inverter is more popular in this application.

Another application is induction cooking. Here, a metal pan replaces the metal piece of the induction heating, and the switching frequency is approximately 20 to 40 kHz.

LOAD-RESONANT DC-TO-DC CONVERTERS

A load-resonant dc-to-dc converter is realized by rectifying the HF ac output of the resonant inverter and then filtering to obtain a smooth dc output. The three most popular half-

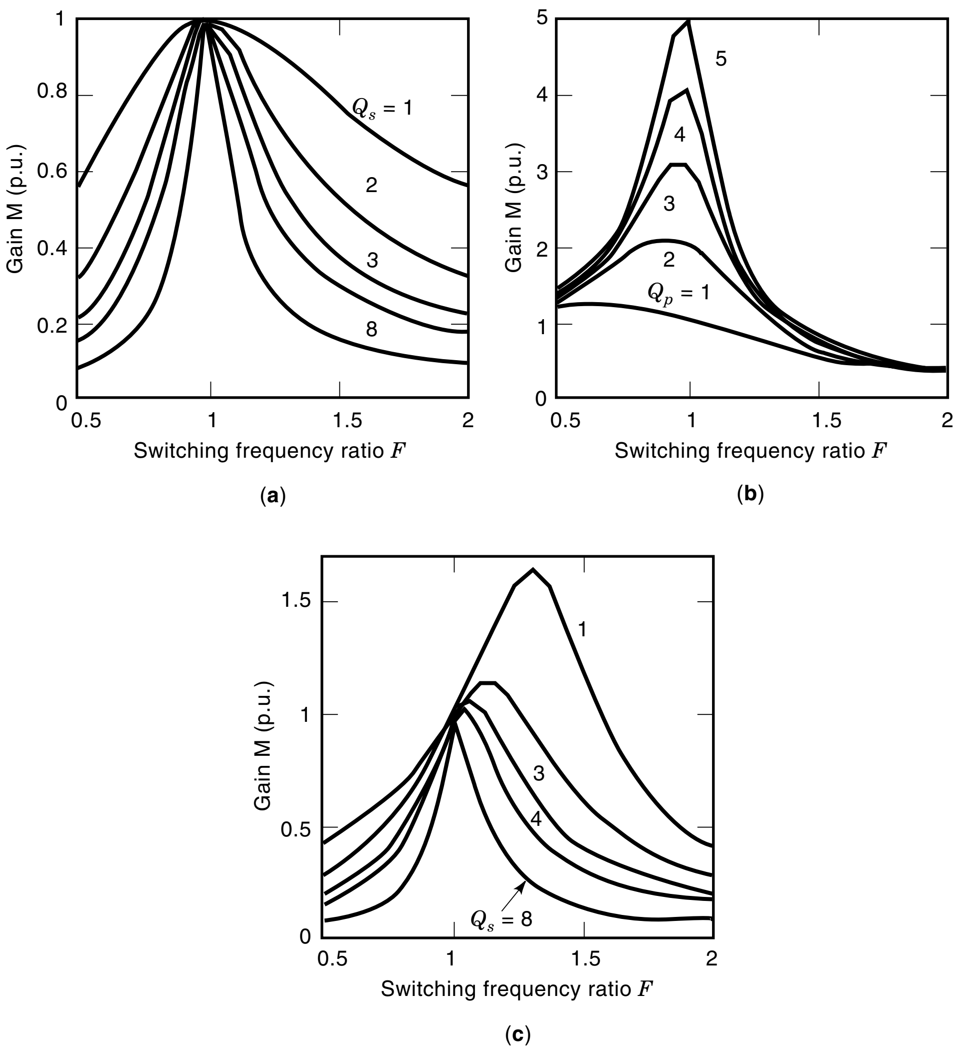

Figure 8. Load resonant inverter gain vs switching frequency ratio F for (a) series-loaded inverter, (b) parallel-loaded inverter, and (c) series-parallel inverter ($C_s/C_p = 1$).

bridge versions of dc-to-dc load-resonant converter configurations (4–6), namely, the series-resonant converter (SRC), the parallel resonant converter (PRC) and the series-parallel resonant converter (SPRC) (also called LCC-type PRC) are shown in Figs. 9(a–c). A capacitive output filter (C_F) is used in the case of the SRC, and an inductive output filter (L_F) is used for the PRC and the SPRC. For power levels of more than 500 W to 1 kW, full-bridge configurations are usually used.

Load voltage is regulated in such converters for input supply variation and load changes by varying the switching frequency or using fixed-frequency (variable pulse width) control. The latter type of control is easy to implement (2) with full-bridge converters.

Series-loaded resonant converters [Fig. 9(a)] are highly efficient from full load to part load. Transformer saturation is avoided because of the series-blocking resonating capacitor. The major problems with the SRC are (1) it requires a very wide change in switching frequency to regulate the load voltage and (2) the output filter capacitor must carry high ripple current (a major problem especially in low-output voltage, high-output current applications).

Parallel-loaded resonant converters [Fig. 9(b)] are suitable for low-output voltage, high-output current applications because of the filter inductance at the output and low ripple current requirements for the filter capacitor. The major disadvantage of the PRC is that the device currents do not decrease with the load current which reduces efficiency at reduced load currents.

The SPRC [Fig. 9(c)] combines the characteristics and desirable features of SRC and PRC.

Higher order resonant converter topologies with improved characteristics have been realized and many of them are presented in (6). Recently, modified series resonant converters (8,9) have been proposed and have drawn the attention of many researchers. These configurations give almost the same performance as the PWM converters but with reduced losses.

Variable Frequency Operation

As explained for resonant inverters, depending on whether the switching frequency is below the natural resonance frequency ω_r or above ω_r, the converter can operate in two different operating modes: (1) Below-Resonance (Leading PF) Mode and (2) Above-Resonance (Lagging PF) Mode. The operating principles, the advantages and disadvantages are the same as those explained previously.

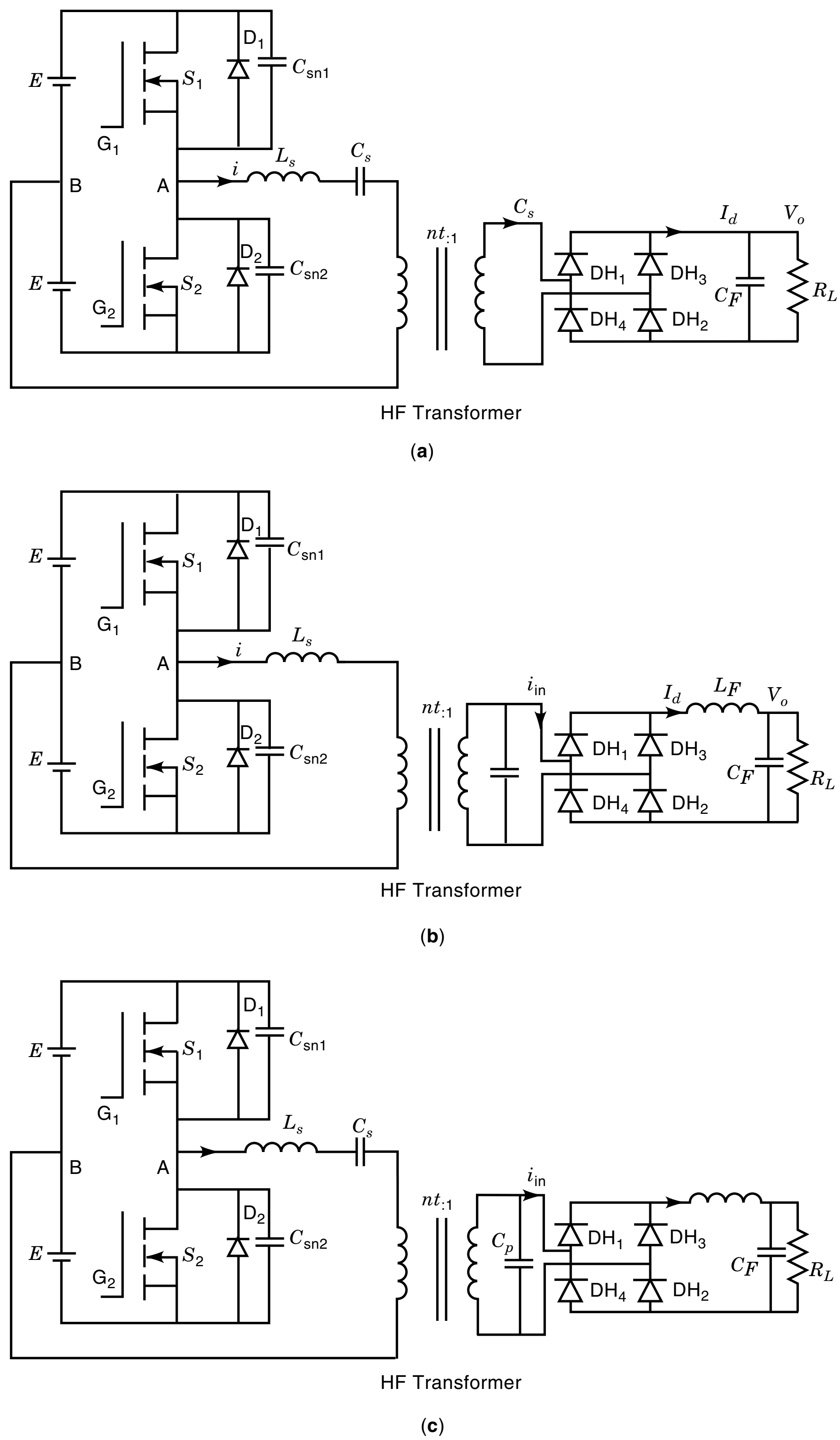

Figure 9. Dc-to-dc load resonant converter (half-bridge version) configurations suitable for operation above resonance. C_{sn1} and C_{sn2} are the snubber capacitors. (a) Series resonant converter. (b) Parallel resonant converter. (c) Series-parallel (or LCC-type) resonant converter. The capacitor C_p is placed on the secondary-side of the HF transformer in (b) and (c) so that the leakage inductances of the HF transformer are part of resonant inductance. For operation below resonance, di/dt limiting inductors and RC snubbers are required. For operation above resonance, only capacitive snubbers are required as shown.

Some of the problems associated with variable-frequency control technique are that variation in switching frequency required for power control is wide for some configurations (e.g., SRC); design of magnetics and filter elements is difficult; and the size of magnetics becomes large when operated below resonance.

Fixed-Frequency Operation

Some of the problems associated with the variable-frequency control of resonant converters are overcome by fixed-frequency operation (9,10). A number of configurations and control methods for fixed-frequency operation are available in the literature [Ref. 10 gives a list of papers]. Among them, most popular method of control is phase-shift control (also called clamped mode or PWM operation). Figure 10(b) illustrates the clamped mode fixed-frequency operation of the SPRC shown in Fig. 10(a). Load power control is achieved by changing the phase-shift angle ϕ between the gating signals to vary the pulse width δ of v_{AB}. Depending on the load current and pulse width δ, the converter operates in several modes: (a) All switches operate with ZVS. (b) Two switches operate with ZVS and two switches operate in ZCS [Fig. 10(b)]. (c) All switches operate in ZCS (at very light load conditions). The fixed-frequency LCL-type resonant configuration proposed in (9) operates in ZVS for all switches over a very wide load variation.

Exact analysis of resonant converters is difficult because of the nonlinear loading on the resonant tanks. The rectifier-filter-load resistor block can be replaced by a square-wave voltage source [for SRC, Fig. 11(a)] or a square-wave current source [for PRC and SPRC, Fig. 11(c) shows the constant current models for the PRC] as explained next.

Because of the use of full-wave rectifier at the output (therefore, this type of resonant converter is also called a double-ended resonant converter), the lowest harmonic frequency component at the output is twice the switching frequency ($2f_s$). In the case of SRC, the resonant current is rectified and filtered by C_F. The output filter capacitor C_F, is large enough to assume that the load voltage is constant. Therefore, the rectifier input voltage is a square-wave of amplitude V_O. When the resonant current i is positive, output diodes DH_1 and DH_2 conduct. Similarly, DH_3 and DH_4 conduct for the negative cycle of i. For analytical purposes, the rectifier, filter, and load can be replaced by a square-wave voltage-source v_O' [Fig. 11(a)] whose phase with respect to square-wave voltage v_{AB} is not known and has to be determined analytically.

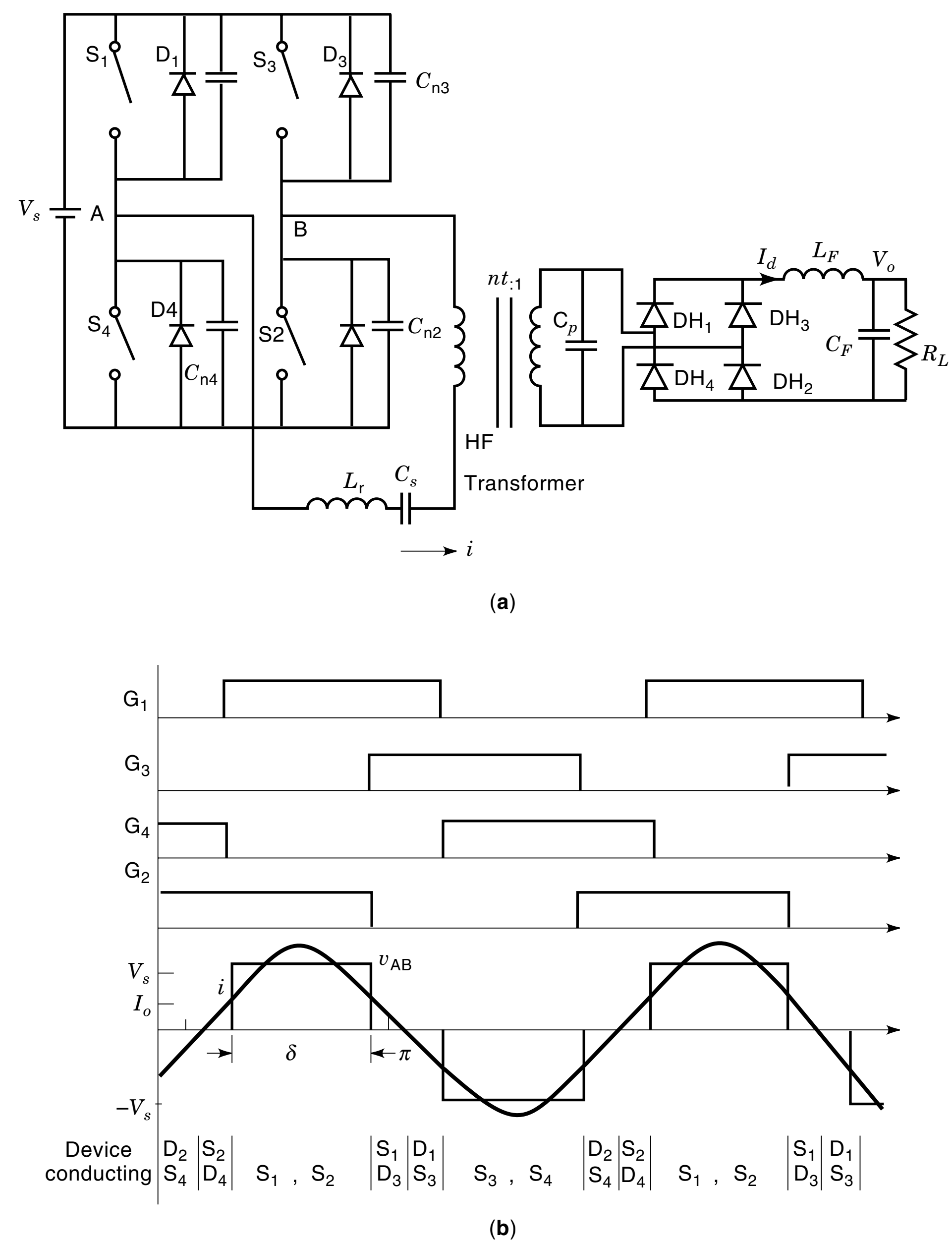

Figure 10. (a) Basic circuit diagram of the series-parallel (LCC-type) resonant converter suitable for fixed-frequency operation with PWM (clamped-mode) control (from Ref. 10, © 1992 IEEE). (b) Typical waveforms to illustrate the operation of a fixed-frequency PWM LCC-type resonant converter working with a pulsewidth δ (from Ref. 10, © 1992 IEEE).

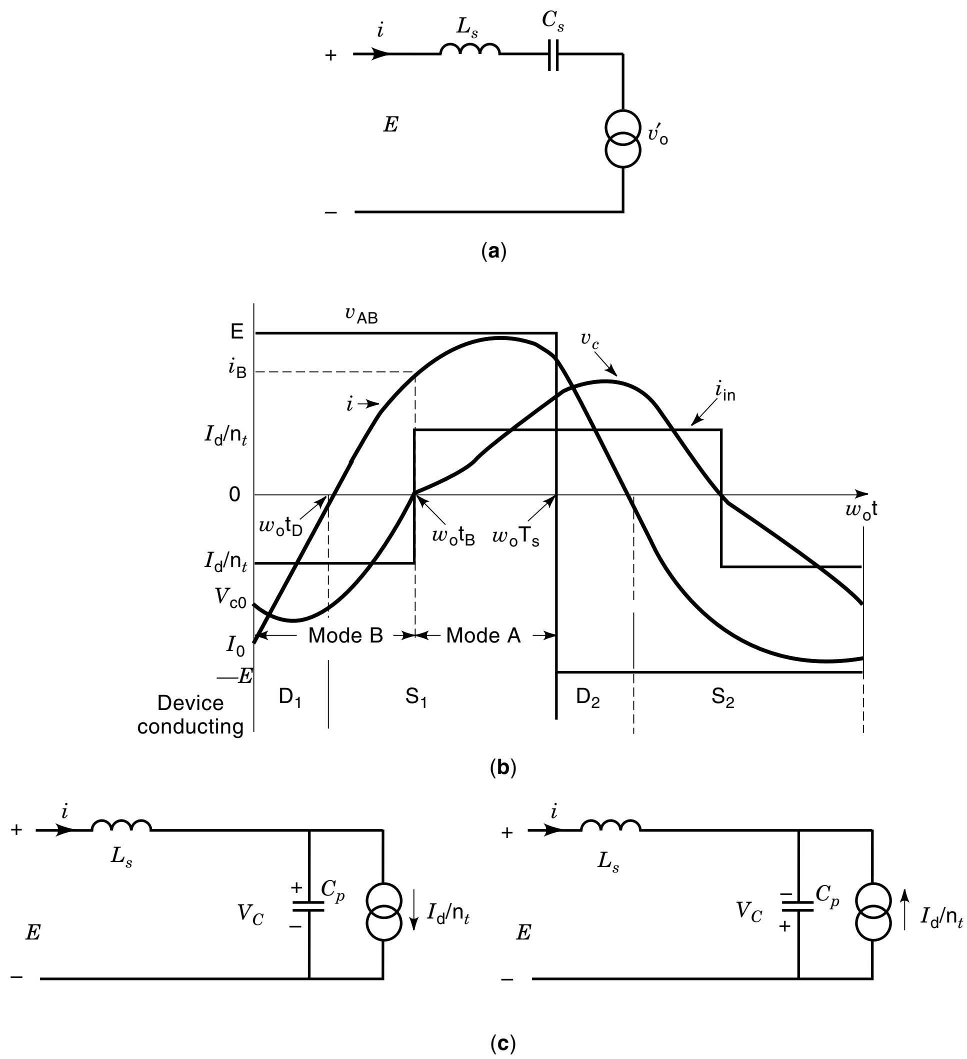

Figure 11. (a) Voltage source model for the SRC of Fig. 9(a). (b) Waveforms at different points in the PRC circuit of Fig. 9(b) for operation above resonance (from Ref. 11, © 1989 IEEE). (c) Constant current models for different operating modes used to analyze the PRC: (i) mode A operation; (ii) mode B operation (from Ref. 11, © 1989 IEEE).

In the case of the PRC and SPRC, the voltage across the capacitor C_p is rectified and filtered, and the current through the filter inductor L_F can be assumed to be constant. With the same logic used for the SRC, the output rectifier, filter inductor, and load for the PRC and SPRC can be replaced by a square-wave current source [shown for the PRC in Fig. 11(c))].

Resonant converters are analyzed by the following three methods:

1. Differential equations (or state-space) approach: This method is difficult for higher order circuits, but gives more exact results. This method is also useful for dynamic analysis [large-signal (12) and small-signal analysis (13–15)] of resonant converters. In this method, differential equations for different intervals of operation are written using the constant current model or constant voltage model discussed earlier. These equations are solved for the various state variables. Closed-form solutions are possible by matching the boundary conditions of the state variables. For example, Fig. 11(b) shows the typical operating waveforms for the PRC of Fig. 9(b), and the constant current model that can be used for the analysis during the two intervals (mode B and mode A) is shown in Fig. 11(c). Using these models, it is possible to obtain closed-form solutions for the PRC as presented in (11). However, closed-form solutions cannot be obtained for higher order topologies or for various modes of operation (for example, the discontinuous capacitor voltage mode for SPRC).

   For transient analysis, the output voltage/current cannot be assumed constant and the output filter elements are also treated as state variables, which increases the number of differential equations. Large-signal analysis is useful for predicting the transient behavior of resonant converters for large step changes in variables like supply voltage or load. The behavior of resonant converters for small perturbations in variables (for example, switching frequency) is studied by small-signal analysis.
2. Fourier Series Approach: In this method, the inverter output voltage and the rectifier input square-wave voltage (or current) are expressed in the Fourier series form. A generalized analysis of resonant dc-to-dc converters using a two-port model and the Fourier series approach is given in (16). The various waveforms for the converter are predicted more accurately (compared with approximate analysis) by this method.

3. Approximate Analysis: Using fundamental components of the waveforms, an approximate analysis (4,6,7,8,10) with a phasor circuit gives a reasonably good design approach. This analytical approach is illustrated for the SPRC in the next section.

Methods 2 and 3 give only steady-state analysis. The describing function method (15) is an approximate but powerful method for the small-signal analysis of resonant converters.

Approximate Analysis of SPRC. Using the fundamental waveforms, the rectifier-filter-load block in Fig. 9(c) is replaced by an equivalent ac resistance R_{ac} $(= (\pi^2/8)R_L')$. Figure 12 shows the equivalent circuit at the output of the inverter. Now the analytical method using this phasor circuit is same as that discussed previously. The same base quantities given there are used for normalization.

For an SPRC, the converter gain [normalized per unit (p.u.) output voltage] referred to the primary side is given by (4,6)

$$M = \sin(\delta/2)/\{(\pi^2/8)^2[1 + (C_p/C_s)(1 - F_s^2)]^2 + Q_s^2[F_s - (1/F_s)]^2\}^{1/2} \quad \text{p.u.} \tag{12}$$

where $\delta = \pi$ for variable-frequency operation,

$$Q_s = (L_s/C_s)^{1/2}/R_L' \tag{13}$$

$$F_s = f_s/f_r \tag{14}$$

f_s = switching frequency, L_s includes leakage inductance of the HF transformer, and

$$f_r = \text{series resonance frequency} = \omega_r/(2\pi) = 1/[2\pi(L_sC_s)^{1/2}] \tag{15}$$

The peak inverter output (same as the resonant inductor and the switch) current is given by

$$I_p = 4/[\pi|Z_{eq}|] \quad \text{p.u.} \tag{16}$$

where Z_{eq} is the equivalent impedance looking at the terminals AB given by

$$Z_{eq} = [B_1 + jB_2]/B_3 \quad \text{p.u.} \tag{17}$$

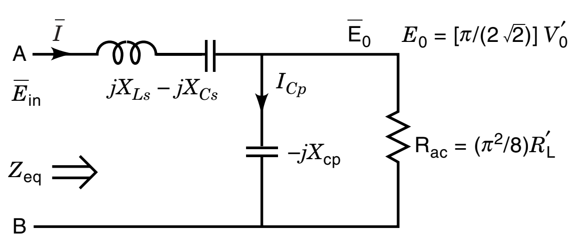

Figure 12. Phasor circuit model used for the approximate analysis of the SPRC converter. $R_{ac} = (\pi^2/8)R_L'$ where $R_L' = n_t^2R_L$. For voltage-source load [e.g., SRC of Fig. 10(a)] $R_{ac} = (8/\pi^2)R_L'$.

where

$$B_1 = (8/\pi^2)(C_s/C_p)^2(Q_s/F_s)^2 \tag{18}$$

$$B_2 = Q_s[F_s - (1/F_s)][1 + (8/\pi^2)^2(C_s/C_p)^2(Q_s/F_s)^2] - (C_s/C_p)(Q_s/F_s) \tag{19}$$

and

$$B_3 = 1 + (8/\pi^2)^2(C_s/C_p)^2(Q_s/F_s)^2 \tag{20}$$

The value of the initial current I_0 is given by

$$I_0 = I_p \sin(-\phi) \quad \text{p.u.} \tag{21}$$

where

$$\phi = \tan^{-1}(B_2/B_1) \quad \text{rad.} \tag{22}$$

The converter is operating in the lagging PF mode if the initial current I_0 is negative. The peak voltage across the capacitor C_p (on the secondary side) is given by

$$V_{cpp} = (\pi/2)V_o \quad \text{V} \tag{23}$$

The peak voltage across C_s and the peak current through C_p are given by

$$V_{csp} = (Q_s/F_s).I_p \quad \text{p.u.} \tag{24}$$

$$I_{cpp} = V_{cpp}/(X_{ctpu}.R_L) \quad \text{A} \tag{25}$$

where

$$X_{cppu} = (C_s/C_p)(Q_s/F_s) \quad \text{p.u.} \tag{26}$$

Using Eq. (12), the plot of converter gain versus the switching frequency ratio F_s is obtained. If the ratio C_s/C_p increases, then the converter takes the characteristics of SRC and the load voltage regulation requires very wide variation in the switching frequency. Lower values of C_s/C_p takes the characteristics of a PRC. Therefore, a compromise value of C_s/C_p = 1 is usually chosen to design such converters (4,6).

The previous approach to derive converter gain and other equations can be repeated (6,7) for the SRC, PRC, and other resonant converters.

The load resonant converters previously described form one class of soft-switching resonant converters. There are two more members of this family, quasi-resonant converters and resonant transition converters, discussed in the next two sections, respectively.

QUASI-RESONANT CONVERTERS

Double-ended, half-bridge or full-bridge load resonant converter configurations discussed earlier are usually used for power levels above 300 W. For lower power levels, quasi-resonant converters (QRC) generated by adding LC elements in single-ended PWM converters (for example, buck, boost, flyback) are used.

Single-Ended or Quasi-Resonant Converters

These converters generate quasi-sinusoidal voltage (or current) waveforms and hence the name quasi-resonant convert-

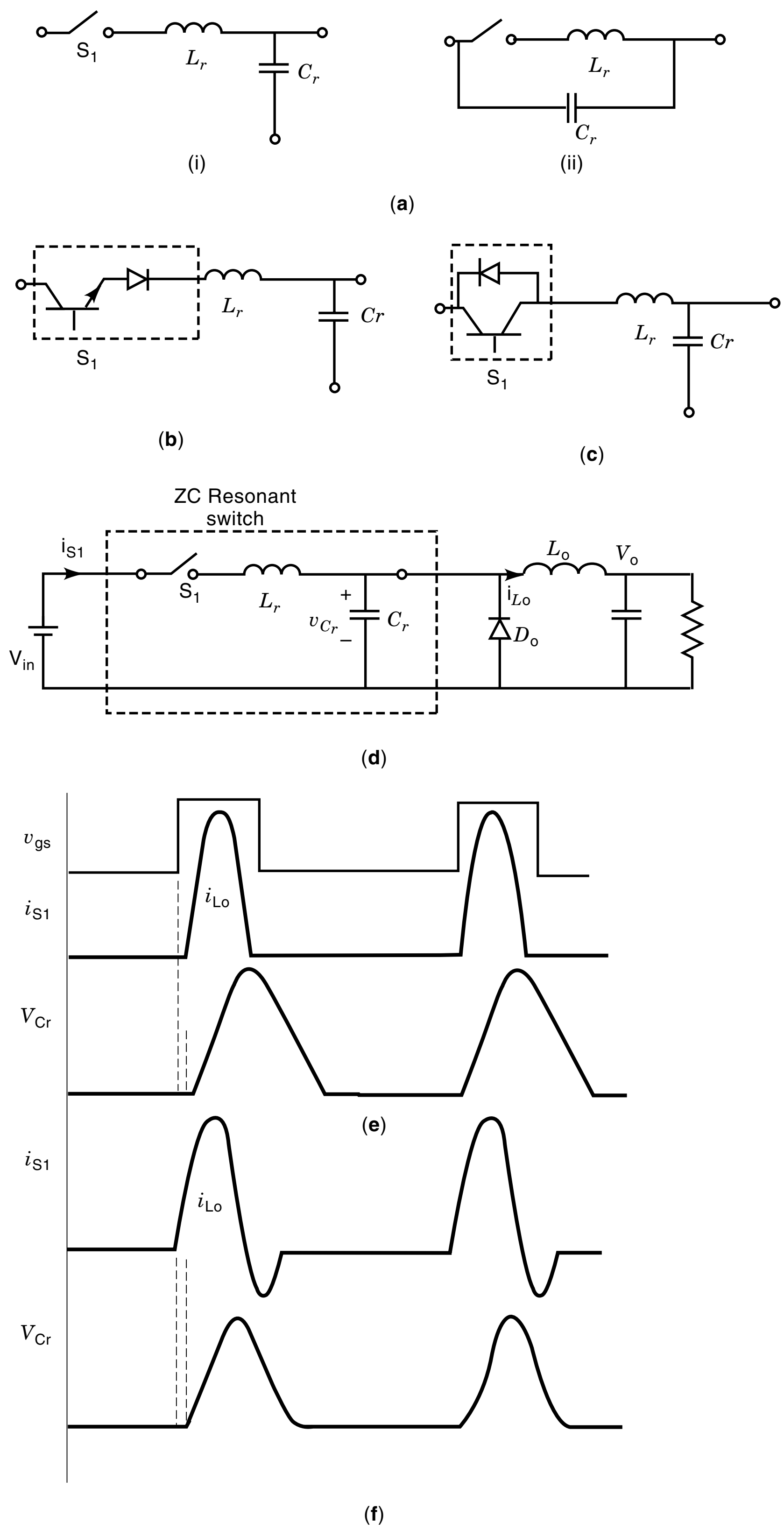

Figure 13. (a) Zero-current resonant switch (i) L-type (ii) M-type. (b) Half-wave configuration using L-type ZC resonant switch. (c) Full-wave configuration using L-type ZC resonant switch. (d) Implementation of ZCS QR buck converter using L-type resonant switch. (e) Operating waveforms for half-wave mode. (f) Operating waveforms for full-wave mode (from Ref. 17, © 1985 IEEE).

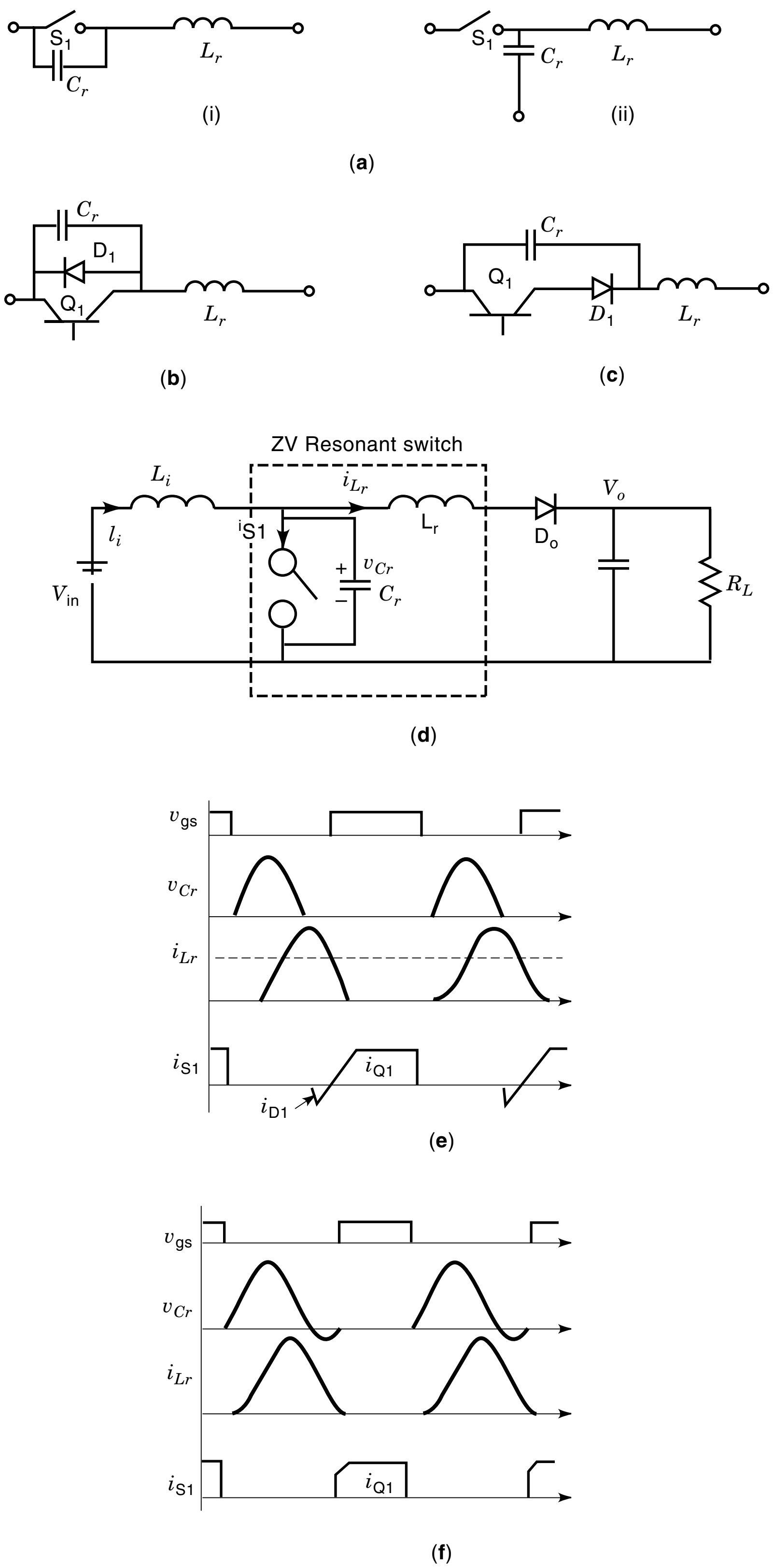

Figure 14. (a) Zero-voltage resonant switches. (b) Half-wave configuration using ZV resonant switch shown in Fig. 14(a)(i) (c) Full-wave configuration using ZV resonant switch shown in Fig. 14(a)(i). (d) Implementation of ZVS QR boost converter using resonant switch shown in Fig. 14(a)(i). (e) Operating waveforms for half-wave mode. (f) Operating waveforms for full-wave mode (from Ref. 18, © 1986 IEEE).

ers (QRC). They operate with zero-current switching (ZCS) or zero-voltage switching (ZVS). The QRC configurations are generated by replacing the switches in conventional PWM switch-mode converters by the resonant switches shown in Figs. 13(a) and 14(a). A number of topologies are realizable. Basic principles of ZCS and ZVS are explained briefly here.

Zero-Current-Switching QRCs

An example of a ZCS QR buck converter implemented with a ZC resonant switch is shown in Fig. 13(d) (17). When a half-wave type resonant switch [Fig. 13(b)] is used, the resonant current (i_{Lr}) is a half sine-wave [Fig. 13(e)] and a full-wave type resonant switch [Fig. 13(c)] generates a full sine-wave [Fig. 13(f)]. The switching device currents are sinusoidal, and therefore, the switching losses are almost negligible with low turn-on and turn-off stresses. ZCS QRCs operate at frequencies of the order of 2 MHz, but they suffer from high peak currents through the switch and capacitive turn-on losses. IGBTs are the preferred devices in ZCS converters because of their low on-state voltage drop.

Zero-Voltage-Switching QRCs

In these converters, the power semiconductor switch turns on at zero voltage (18). This condition is created by shaping its off-time voltage waveform by adding the auxiliary LC elements. An example of ZVS QR boost converter implemented using a ZV resonant switch is shown in Fig. 14(d). The circuit operates in the half-wave mode [Fig. 14(e)] or in the full-wave mode [Fig. 14(f)] depending on whether a half-wave [Fig. 14(b)] or full-wave [Fig. 14(c)] ZV resonant switch is used, and the name comes from the capacitor voltage (v_{Cr}) waveform. The full-wave mode ZVS circuit suffers from capacitive turn-on losses. The major problem with ZVS QRCs is the increased voltage stress across the switch. However, ZVS QRCs are operated at much higher frequencies compared with ZCS QRCs. Variable frequency control is used for power control in QRCs. Fixed-frequency control is realized by adding extra power switches.

RESONANT TRANSITION CONVERTERS

From the principles presented in the earlier sections, it can be observed that the resonant converters suffer from high current (or voltage) stress across the switches caused by the generation of sinusoidal currents (and voltages). To overcome this problem, recently, resonant transition converters have been proposed (19,20). These converters use LC elements together with an auxiliary switch (whose rating is much lower than the main switch) in parallel with the main switching device. Resonant transitions are used only during switching instants. The following are two possible types of converters:

Zero-Current Transition PWM Converters

An example of a zero-current transition boost converter is shown in Fig. 15. More details of operation are in reference (19). A major problem is the switch capacitance discharge current through the switch at turn-on, which is common for ZCS converters. In addition, at turn-on, there is an extra current due to the stored energy in the LC circuit. Because the turn-off tail current is removed, this configuration is attractive in high power converters when IGBTs or bipolar transistors are used as the switching devices.

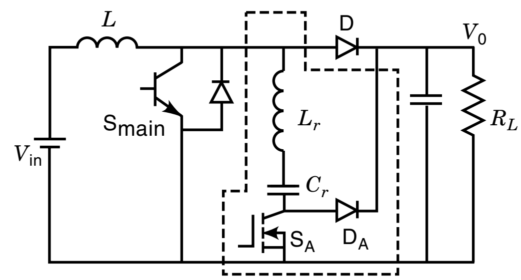

Figure 15. Zero-current-transition PWM boost converter. Elements shown in dashed lines are added to the original PWM boost converter (from Ref. 19, © 1993 IEEE).

Zero-Voltage Transition PWM Converters (20)

An example of a zero-voltage transition boost converter is shown in Fig. 16. The function of auxiliary switch S_A is to create a ZVS condition for the main switch at turn-on. Some of the problems are that the auxiliary switch turns off like a PWM switch, and the inductor L_r and the switched-capacitance of S_A generate ringing when S_{main} is on. The latter problem is solved by a saturable inductor or a damping circuit.

In spite of some of the disadvantages mentioned, these converters have the following advantages: fixed-frequency ZCS or ZVS PWM operation with characteristics closer to the PWM converters; operation in ZCS or ZVS for both the switches and rectifier diodes for wide load and line voltage variations. But the leakage inductance of the HF transformer must be minimized in the isolated version of the converters. Extra components and drive circuits are also required.

A widely used full-bridge, fixed-frequency ZVS PWM converter (21,22) operates with ZVT during the switching instants. In Fig. 10(a), if C_p is removed and C_s is large, this configuration results. This converter has characteristics similar to a PWM converter with approximate square-wave currents, but operates with ZVS. The gating signals are phase-shifted as shown in Fig. 10(b) to generate a quasi-square wave across AB. Similar to the load-resonant ZVS converters, the snubber capacitor is discharged and the inverse-parallel diode across the switch is turned on before turning on the switch. The function of C_s is to block any dc current flowing through the HF transformer. The inductance L_s is the leakage inductance of the HF transformer plus any external inductance added. Inductor L_s plays an important role. The stored energy in this inductor must be larger than the snubber ca-

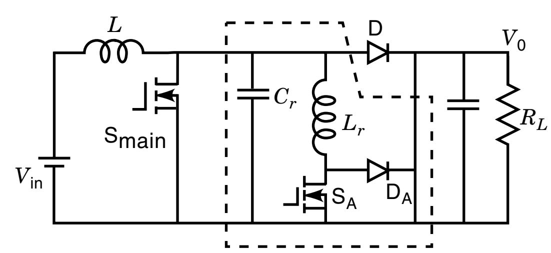

Figure 16. Zero-voltage-transition PWM boost converter. Elements shown in dashed lines are added to the original PWM boost converter (from Ref. 20, © 1992 IEEE).

pacitive energy to charge/discharge the snubber capacitors and to ensure ZVS for wide load range. On the other hand, if the inductor is too large, it may take too long to reach the required load current within the switching cycle. This also reduces output voltage because of the duty ratio loss. Based on these constraints, design methods are given in (21,22). It is difficult to achieve ZVS at light load conditions. Recently, this configuration has drawn the attention of researchers and many improved versions have been published. There are some integrated circuits available for generating the gating signals required for the ZVS PWM converter, for example, Unitrode UC3875 (22).

Another modified PWM converter is the pseudoresonant dc/dc converter discussed in (23). Dc link resonant converters are used mainly in high-power applications (for example, in motor drives), and they use the resonant circuit at the input side to create ZVS condition for the single-phase or three-phase bridge circuit. Usually, such converters do not provide HF transformer isolation. This configuration is explained well in (24).

More details are in a number of references listed in the Bibliography.

BIBLIOGRAPHY

1. R. Severns and G. Bloom, *Modern Switching dc-to-dc Converters,* New York: Van Nostrand, 1988.
2. S. B. Dewan and A. Straughen, *Power Semiconductor Circuits,* New York: Wiley, 1984.
3. A. K. S. Bhat and S. B. Dewan, A generalized approach for the steady-state analysis of resonant inverters, *IEEE Trans. Ind. Appl.,* **35**: 326–338, 1989.
4. R. L. Steigerwald, A comparison of half-bridge resonant converter topologies, *IEEE Trans. Power Electron.,* **PE-3**: 174–182, 1988.
5. R. L. Steigerwald, High frequency resonant transistor dc/dc converters, *IEEE Trans. Ind. Electron.,* **31**: 181–191, 1984.
6. A. K. S. Bhat, A unified approach for the steady-state analysis for resonant converters, *IEEE Trans. Ind. Electron.,* **38**: 251–259, 1991.
7. M. K. Kazimierczuk and D. Czarkowski, *Resonant Power Converters,* New York: Wiley, 1995.
8. A. K. S. Bhat, Analysis and design of LCL-type resonant converter, *IEEE Trans. Ind. Electron.,* **41**: 118–124, 1994.
9. A. K. S. Bhat, A fixed-frequency modified series-resonant converter: Analysis, design and experimental results, *IEEE Trans. Power Electron.,* **10**: 766–775, 1995.
10. A. K. S. Bhat, Fixed frequency PWM series-parallel resonant converter, IEEE Ind. Appl. Conf. Record, *IEEE Trans. Ind. Appl.,* **28**: 1002–1009, 1992.
11. A. K. S. Bhat and M. M. Swamy, Analysis of parallel resonant converter operating above resonance, *IEEE Trans. Aerosp. Electron. Syst.,* **25**: 449–458, 1989.
12. V. Agarwal and A. K. S. Bhat, Large signal analysis of the LCC-type parallel resonant converter using discrete time domain modeling, *IEEE Trans. Power Electron.,* **10**: 222–238, 1995.
13. V. Agarwal and A. K. S. Bhat, Small signal analysis of the LCC-type parallel resonant converter using discrete time domain modeling, *IEEE Trans. Ind. Electron.,* **42**: 604–614, 1995.
14. I. Baterseh and K. Siri, Generalized approach to the small signal modeling of dc-to-dc resonant converters, *IEEE Trans. Aerosp. Electron. Syst.,* **29**: 894–908, 1993.
15. E. X. Yang, F. C. Lee, and M. M. Jovanovic, Small-signal modeling of series and parallel resonant converters, *IEEE PESC,* Toledo, Spain, 1992, pp. 785–792.
16. A. K. S. Bhat, A generalized steady-state analysis of resonant converters using two-port model and Fourier series approach, *IEEE Applied Power Electron. Conf.,* Dallas, March 1995, pp. 920–926.
17. K. H. Liu, R. Oruganti, and F. C. Lee, Resonant Switches—Topologies And Characteristics, *IEEE Power Electron. Specialists Conf. Record,* Toulouse, France, 1985, pp. 106–116.
18. K. H. Liu and F. C. Lee, Zero-Voltage Switching Technique In dc/dc Converters., *IEEE Power Electron. Specialists Conf. Record,* Vancouver, 1986, pp. 58–70.
19. G. Hua, E. X. Yang, Y. Jiang, and F. C. Lee, Novel zero-current-transition PWM converters, *IEEE PESC,* Seattle, WA, 1993, pp. 538–543.
20. G. Hua, C. S. Leu, and F. C. Lee, Novel zero-voltage-transition PWM converters, *IEEE PESC,* Toledo, Spain, 1992, pp. 55–61.
21. D. B. Dalal, A 500 kHz multi-output converter with zero voltage switching, *IEEE Appl. Power Electron. Conf. Record,* Los Angeles, 1990, pp. 265–274.
22. Unitrode Corporation, *Integrated Circuits and Applications Handbook,* Merrimack, NH, 1995–96.
23. O. D. Patterson and D. M. Divan, Pseudo-resonant full bridge dc/dc converter, *IEEE PESC,* Blacksberg, VA, 1987, pp. 424–430.
24. D. M. Divan, The Resonant dc Link Converter—A New Concept in Power Conversion, *IEEE IAS Record,* Denver, CO, 1986, pp. 648–656.

Reading List

J. G. Kassakian, M. F. Schlecht, and G. C. Verghese, *Principles of Power Electronics,* Reading, MA, Menlo Park, CA: Addison–Wesley, 1991.

K. Kit Sum, *Recent Developments in Resonant Power Conversion,* Intertech Communications Inc., CA, 1988. [This book contains a collection of selected papers on resonant converters.]

N. Mohan, T. M. Undeland, and W. R. Robins, *Power Electronics—Converters, Applications, and Design,* New York: Wiley, 1995.

ASHOKA K. S. BHAT
University of Victoria